Microwave-assisted synthesis of Sb_2Se_3 submicron rods, compared with those of Bi_2Te_3 and Sb_2Te_3

2009 Nanotechnology 20 085604

(http://iopscience.iop.org/0957-4484/20/8/085604)

Nanotechnology **20** (2009) 085604 (6pp) doi:10.1088/0957-4484/20/8/085604

Microwave-assisted synthesis of Sb_2Se_3 submicron rods, compared with those of Bi_2Te_3 and Sb_2Te_3

Bo Zhou[1,2] **and Jun-Jie Zhu**[2,3]

[1] Jiangsu Key Laboratory of Biofunctional Materials, College of Chemistry and Environmental Science, Nanjing Normal University, Nanjing 210097, People's Republic of China
[2] Key Laboratory of Analytical Chemistry for Life Science (MOE), School of Chemistry and Chemical Engineering, Nanjing University, Nanjing 210093, People's Republic of China

E-mail: zhb_zhou@tom.com and jjzhu@nju.edu.cn

Received 31 October 2008, in final form 12 December 2008
Published 2 February 2009
Online at stacks.iop.org/Nano/20/085604

Abstract
Orthorhombic Sb_2Se_3 submicron rods were prepared from antimony sodium tartrate and Se powder via a microwave-assisted chemical method. The products were characterized by x-ray powder diffraction (XRD), transmission electron microscope (TEM) and selected-area electron diffraction (SAED) techniques. The reaction mechanism and the morphology of the product were studied in detail in comparison with those in the syntheses of Bi_2Te_3 and Sb_2Te_3. The synthesis of Sb_2Se_3 was based on the polyol reducing process and microwaves played an important role. The morphologies of the compounds were mainly determined by their inherent anisotropic crystal structures. The optical properties of as-prepared Sb_2Se_3 were also characterized by UV–vis diffuse reflectance spectroscopy, and the bandgap (E_g) can be derived to be 1.16 eV, which is suitable for applications in photovoltaic conversion.

1. Introduction

One-dimensional (1D) semiconductor nanomaterials (and submicron materials), including nanorods, nanowires, nanotubes and nanoribbons, have attracted a great deal of attention because of their distinctive electronic, optical, mechanical and other properties that differ from those of the bulk materials, and their promising applications as building blocks for nanodevices [1–6]. Employing hard templates or soft structure directors is a widely used strategy to grow 1D nanostructures [7, 8]. And, as for the materials that have inherent anisotropic structures, 1D nanostructures can also be fabricated based on the natural crystal growth mechanism without using templates or structure directors [9–11].

Antimony triselenide, an important member of V_2VI_3 (V = As, Sb, Bi; VI = S, Se, Te) type main-group metal chalcogenides, is a direct bandgap semiconductor that crystallizes in the orthorhombic system. It exhibits good photovoltaic properties and high thermoelectric power (TEP), which makes it promising for applications in photochemical devices, optical devices and thermoelectric cooling devices [12–16]. Besides these, Platakis *et al* reported threshold and memory switching phenomena on the materials of Sb_2Se_3 [17].

Traditionally, Sb_2Se_3 was prepared by elemental reaction of antimony and selenium at high temperature [18]. Recently, some wet chemical methods have been utilized to synthesize 1D Sb_2Se_3 nanocrystals, such as the colloid route [19] and refluxing reaction [20]. However, the most widely used method is the hydrothermal/solvothermal process [21–28, 13]. Sb_2Se_3 with various 1D structures, such as nanowires [21, 22, 25, 26], nanorods [23, 27], nanoribbons [24, 28] and nanotubes [13], were successfully prepared via this hydrothermal/solvothermal process. In these syntheses, strong reductants, such as $NaBH_4$ [25, 28, 29], NaHSe [30] and Na_2SO_3 [26, 27, 31], were usually used to promote the reactions.

Here, we report a microwave-assisted polyol method for the rapid synthesis of 1D Sb_2Se_3 submicron rods. To the best of our knowledge, there is no other report on the synthesis of 1D Sb_2Se_3 via a microwave chemical method. The raw materials used here are only antimony sodium tartrate, Se powder and ethylene glycol, which acts as both solvent and reductant.

[3] Author to whom any correspondence should be addressed.

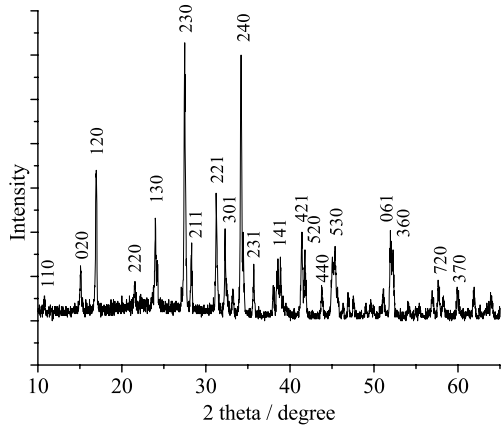

Figure 1. XRD pattern of as-prepared Sb_2Se_3.

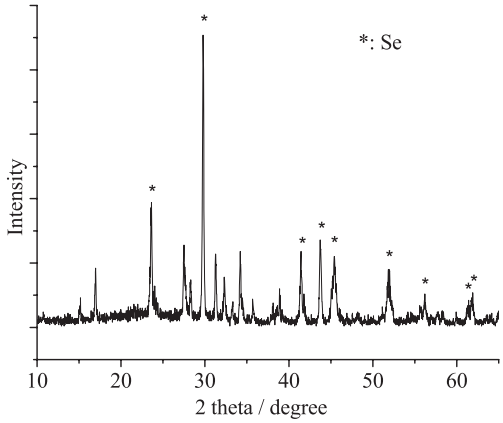

Figure 2. XRD pattern of the sample obtained after 1 h of reaction.

This synthesis was studied in detail in comparison with the syntheses of Bi_2Te_3 and Sb_2Te_3 under similar conditions from the viewpoints of the reaction mechanism and the morphology of the product.

2. Experimental details

All reagents are of analytical purity and were used without further purification. The typical synthesis procedure is as follows: 2 mmol of antimony sodium tartrate ($Na(SbO)C_4H_4O_6$), 3 mmol of Se powder and 30 ml of ethylene glycol (EG) were added to a 100 ml round-bottomed flask, which was then put into a microwave oven equipped with a condenser to carry out the reaction under refluxing. The microwave frequency was 2.45 GHz and the power was set at 280 W. The microwave irradiation time was 3 h. The product was cooled, centrifuged, washed with water and ethanol for several times, and then dried at 60 °C.

The products were characterized by x-ray powder diffraction (XRD) with a Philips X'pert x-ray diffractometer using Cu Kα radiation ($\lambda = 1.5418$ Å). The morphology and the microstructures of the products were investigated by scanning electron microscopy (SEM), transmission electron microscopy (TEM) and selected-area electron diffraction (SAED) with, respectively, a JSM-5610LV (JEOL, 150 kV, WD 10 mm) SEM and a JEM-200CX (JEOL, 200 kV) TEM. The optical properties of the solid product were characterized by a UV–vis diffuse reflectance spectrum and absorbance spectrum using a Varian Cary-5000 UV–vis–NIR spectrophotometer. The TEM image and SAED pattern of the Sb colloid were recorded by H-7650 (Hitachi, 80 kV) TEM and H-600A-2 (Hitachi, 75 kV) EM, respectively.

3. Results and discussion

Experimental results are given below, after which the synthesis mechanism and morphology are discussed, respectively.

3.1. Synthesis mechanism

The typical XRD pattern of as-prepared samples was shown in figure 1. All the diffraction peaks can be indexed to pure orthorhombic Sb_2Se_3 (JCPDS no. 72-1184). No impurities were detected. The sharpness of the peaks indicates the high crystallinity of the sample. The abnormal strengthening of the ($hk0$) diffraction peaks, which is most evidently shown in the (230) and (240) peaks, implies the 1D preferred growth along the (001) direction, which is confirmed by TEM and SAED investigations as discussed below.

This synthesis procedure is similar to that of Bi_2Te_3 [32] and that of Sb_2Te_3 [33]. However, the mechanisms seemed different from each other. As reported previously, the synthesis of Bi_2Te_3 in EG was based on the polyol process, in which Bi(III) was first reduced by EG to metallic Bi, as XRD proved. Then this reduced Bi reacted with Te powder to produce Bi_2Te_3. The synthesis of Sb_2Te_3, as discussed elsewhere [33], was based on the disproportionating reaction of Te, in which Te^{2-} was produced and then reacted with Sb^{III} to produce Sb_2Te_3. However, in the synthesis of Sb_2Se_3, neither reduced Sb was detected by XRD nor was the disproportionation of Se needed.

First, in the synthesis of Sb_2Se_3, no reduced Sb was detected. When the reaction time was not long enough and the reaction was not completed yet, only unreacted Se (the XRD peaks of which were marked with '*' and could be indexed to hexagonal Se, JCPDS no. 06-0362), but no reduced Sb, was found among the produced Sb_2Se_3, as the XRD pattern shown in figure 2 indicates. This result seems to deny the synthesis mechanism based on the reduction of Sb(III), according to which Sb should be detected during the reaction. Two other facts also seemed to confirm this conclusion. One is that, when antimony sodium tartrate was microwave heated in EG without Se, no solid Sb was obtained, no matter if NaOH was added or not. This means that EG was not a strong enough reductant to reduce Sb(III) to solid metallic Sb, though it can reduce Bi(III) to metallic Bi [32]. The other one is that, when Sb powder and Se powder were microwave heated together in EG, almost no Sb_2Se_3 was obtained even after reaction for 3 h. Sb and Se remained unreacted. This means that it is hard for the powders of these two elements to react directly under this condition. The synthesis of Sb_2Se_3 was too slow to be detected.

Second, the synthesis of Sb_2Se_3 is not based on the disproportionation of Se, either. If it were, NaOH would

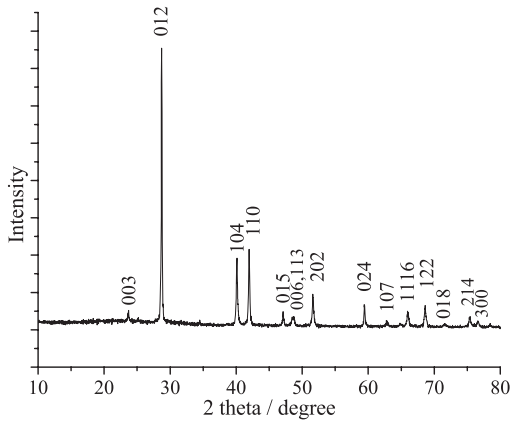

Figure 3. XRD pattern of the sample obtained when NaOH was added.

accelerate the disproportionating reaction and the synthesis of Sb_2Se_3. However, we found that, when NaOH was added to the reaction system, neither Sb_2Se_3 nor Se was obtained. Instead, Sb was found as the only product. This can be seen from the XRD pattern shown in figure 3. All the diffraction peaks can be indexed to hexagonal Sb, JCPDS no. 71-1173. There are three reagents that might reduce antimony: EG, Se and Se^{2-}. Since no solid Sb was obtained without addition of Se or NaOH, as discussed above, we suggest that Se^{2-} was the one that worked. Otherwise, if EG worked, Se should not be necessary; and if Se worked, NaOH should not be necessary. The reduction of antimony is suggested via the following mechanism: firstly, Se disproportions in an alkali medium to give Se^{2-} (equation (1)). Se^{2-} is a reductant even stronger than Zn ($Se + 2e^- = Se^{2-}$, $\varphi^\theta = -0.77$ V; $Zn^{2+} + 2e^- = Zn$, $\varphi^\theta = -0.76$ V), which has been successfully used as a reductant to produce Sb dendrites from antimony sodium tartrate [34]. So, it is reasonable to suggest that Se^{2-} then reduces Sb(III) to metallic Sb (equation (2)):

$$3Se + 6OH^- \rightarrow SeO_3^{2-} + 2Se^{2-} + 3H_2O \quad (1)$$

$$3Se^{2-} + 2Sb^{III} \rightarrow 2Sb + 3Se. \quad (2)$$

The Se produced in equation (2) disproportions again in equation (1). The total reaction can be represented as

$$3Se + 4Sb^{III} + 18OH^- \rightarrow 4Sb + 3SeO_3^{2-} + 9H_2O. \quad (3)$$

So, Sb_2Se_3 was not obtained in the alkali medium.

Absolutely denying the second mechanism which was based on the disproportionation of Se, we are compelled back to the first one, based on the reduction of antimony, because no other mechanism seems more reasonable. Though, as discussed above, no Sb(0) was detected and the first mechanism seems impossible at first sight, when we look further into it, all the facts can be explained.

We suggest that Sb(III) was reduced by EG to give Sb(0). Because the reducing ability of EG is not strong enough, the reduced Sb was very little and very small. In other words, a dilute 'Sb colloid' was produced (equation (4)):

$$Sb(III) + EG \rightarrow Sb(colloid). \quad (4)$$

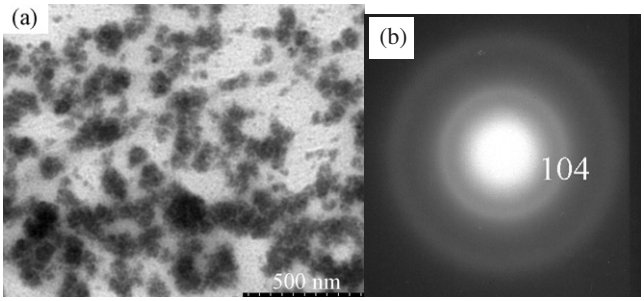

Figure 4. TEM image (a) and SAED pattern (b) of the Sb colloid.

To prove the formation of Sb colloid, we dissolved antimony sodium tartrate in EG and then heated the solution in a microwave oven for 3 h. Though almost no solid was produced, we centrifuged the liquid obtained in a tube. After centrifuging, we inclined the tube very carefully to decant the upper 2/3 of the liquid, then added absolute ethanol into the tube to the original volume. The liquid in the tube was mixed up thoroughly by shaking and ultrasonication, and then was centrifuged again. This cycle was repeated four times. On the last time, most of the liquid was decanted and only ~1 ml was left at the bottom, from which the sample for TEM observation was made. Figure 4 shows the TEM image and the SAED pattern of the sample. Most of the particles were of diameters smaller than 20 nm. The diffraction rings in the SAED pattern indicated their crystallinity. The calculated *d* value was consistent with that of hexagonal Sb (JCPDS no. 71-1173).

This freshly made 'Sb colloid' is much more reactive than Sb powder, and it reacted easily with Se to produce Sb_2Se_3 (equation (5)):

$$2Sb(colloid) + 3Se \rightarrow Sb_2Se_3. \quad (5)$$

Equation (5) is a much faster reaction. The resulting consumption of Sb (colloid) drove equation (4) to the right and thus made the reduction of antimony and the synthesis of Sb_2Se_3 complete.

Because the Sb colloid was produced (via equation (4)) slowly and consumed (via equation (5)) rapidly, it remained as a dilute colloid all through the reaction. Therefore, no evident solid Sb was detected during the reaction. For the same reason, no solid Sb was obtained when antimony sodium tartrate was microwave heated in EG without Se. The fact that Sb powder and Se powder did not react so obviously with each other under similar conditions can be explained as the result of the much lower reactivity of Sb powder than Sb colloid. However, Sb and Se can indeed react to produce Sb_2Se_3, as discussed elsewhere [35].

Other experimental facts also confirm the suggested mechanism. First, when water was used as a solvent to replace EG, no Sb_2Se_3 was obtained, because water has no reducing ability, which is necessary here. Second, Sb_2Se_3 could not be obtained under ultrasonic irradiation instead of microwave irradiation, because the reaction temperature was too low, and thus the reducing ability of EG was restrained.

Another notable fact is that microwaves played an important role in this synthesis of Sb_2Se_3. When the reaction

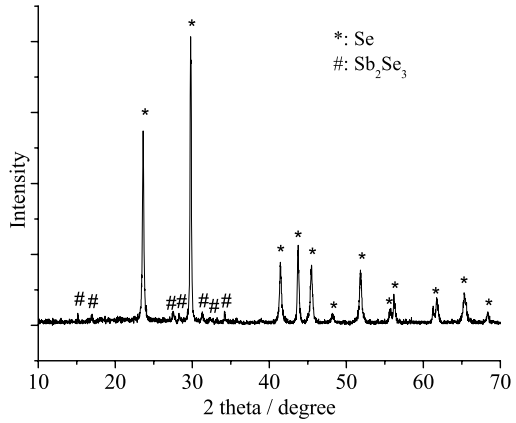

Figure 5. XRD pattern of the sample obtained solvothermally at 180 °C after 30 h of reaction.

was carried out solvothermally at temperatures as high as 180 °C and for times as long as 30 h, which was 10 times that needed under microwave irradiation, a large amount of Se remained unreacted among the produced Sb_2Se_3. This can be seen from the XRD pattern shown in figure 5, in which peaks marked with '#' can be indexed to Sb_2Se_3, and those stronger peaks marked with '*' can be indexed to Se.

3.2. Morphology of as-prepared Sb_2Se_3

The morphology of as-prepared Sb_2Se_3 was investigated with TEM and SAED, and was found to be rod-like as the XRD result implies. From the SEM and TEM images shown in figures 6(a)–(c), it can be seen that these rods were mainly 100–200 nm in diameter, and with lengths ranging from several micrometers to more than ten micrometers. A few of the rods were thicker, with diameters of 400–500 nm. Bright spots in the SAED pattern of an individual rod show the single crystallinity of these rods and can be indexed as shown in figure 6(d). It can be concluded that these submicron rods had preferential growth direction along the (001) direction, which was consistent with the XRD result.

Nonionic, anionic and cationic surfactants, such as polyethylene glycol (PEG-2000), sodium dodecyl sulfonate (SDS), sodium dodecyl benzene sulfonate (SDBS), cetyltrimethyl ammonium bromide (CTAB) and polyvinyl pyrrolidone (PVP, K-30), were added to the reaction system in an attempt to minimize and make the products more uniform. However, no significant difference in morphology was seen. Meanwhile, the reaction was slowed on the addition of some surfactants. For example, when PVP was added, the reaction time should be prolonged to 4.5 h to complete the synthesis. This might be due to the protective adsorption of the surfactant onto the reduced Sb colloid particles.

The difference in morphology between Sb_2Se_3, Sb_2Te_3 and Bi_2Te_3, which were synthesized under similar conditions, is reasonably suggested to result from the difference between their crystal structures. Sb_2Te_3 and Bi_2Te_3 have similar intrinsic anisotropic layered crystal structures [36], in which every 15 layers stacked along the *c* axis and present the combination of three hexagonal layer stacks of composition in which each set consists of five atoms (Te_1–Sb(Bi)–Te_2–Sb(Bi)–Te_1). Between two adjacent Te_1 layers, there are van der Waals bonds, while all others are covalent bonds. This special bonding structure leads

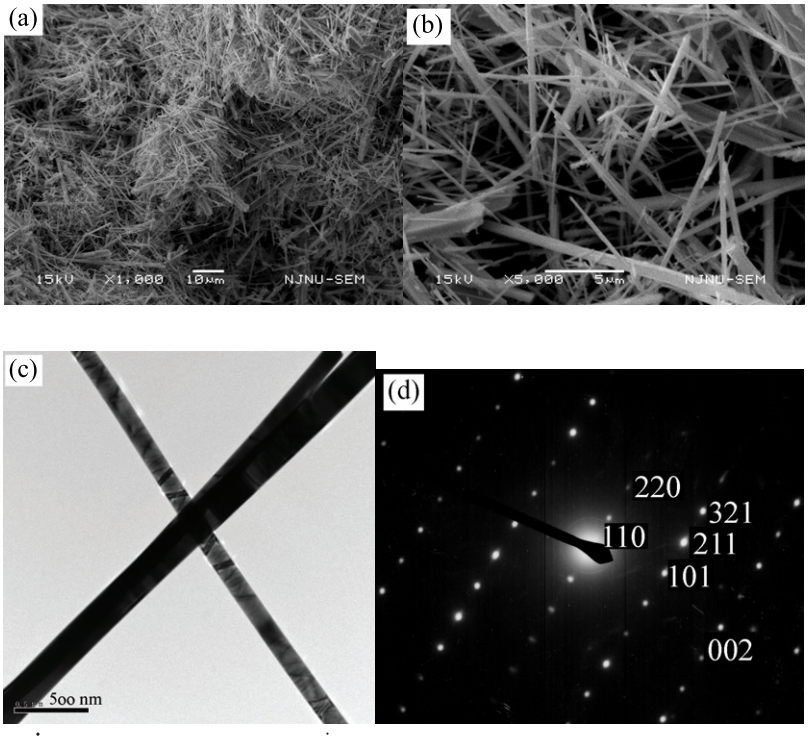

Figure 6. SEM ((a), (b)) and TEM (c) images and SAED pattern (d) of as-prepared Sb_2Se_3.

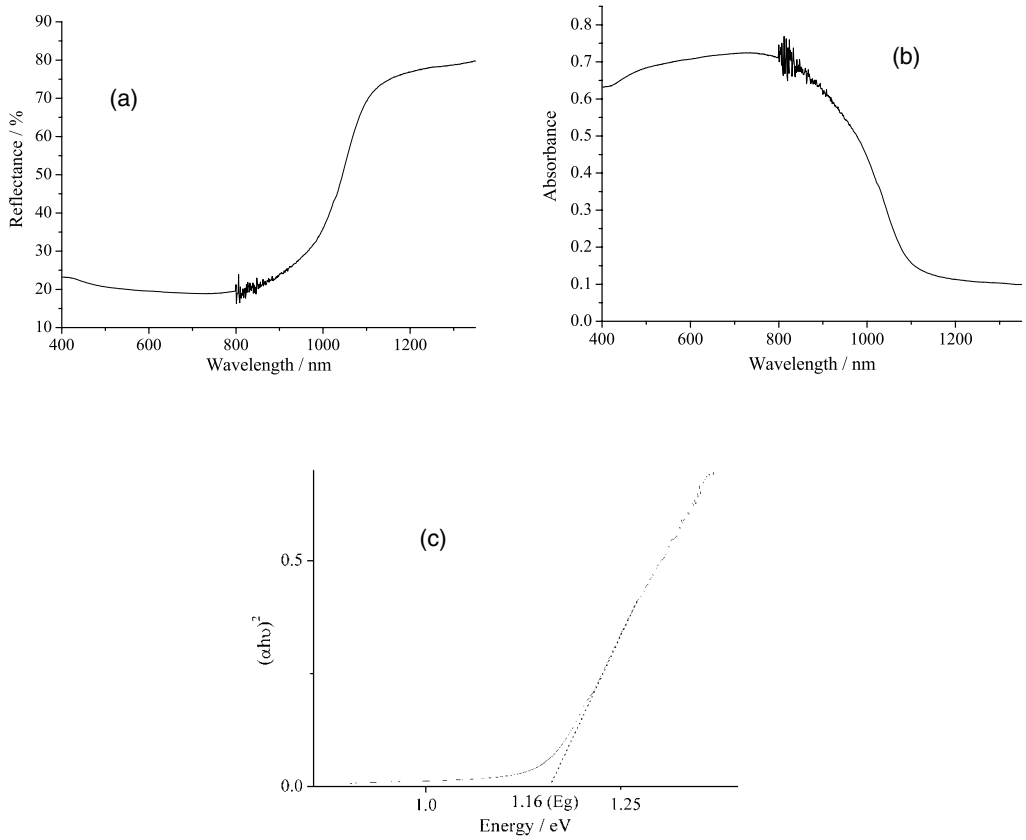

Figure 7. (a) The diffuse reflectance spectrum of as-prepared Sb_2Se_3 submicron rods; (b) the absorbance spectrum corresponding to (a); (c) the plot corresponding to (b), from which the bandgap (E_g) can be derived to be 1.16 eV.

to the faster growth of the crystal along the top–bottom crystalline plane compared with that along the *c* axis, which makes them tend to form a plate-like morphology [37]. The crystal structure of Sb_2Se_3 is rather different. Sb_2Se_3 has an orthorhombic lattice with four molecules per unit cell [38, 39]. Its structure can be thought of as made up of puckered sheets running parallel to the *c* axis. The binding between these sheets is considerably weaker than that within the sheets. Considering the strong Sb–Se bonds, these sheets consist of infinite chains of Sb_2Se_3 parallel to the *c* axis [39]. This suggests that preferential growth occurs in the [001] direction, which leads to the formation of Sb_2Se_3 wires or rods.

The fact that surfactants made no significant difference in the morphologies of the products in all three syntheses indicates that the intrinsic anisotropic crystal structures play a decisive role in their morphologies.

3.3. Optical property of as-prepared Sb_2Se_3

Figures 7(a) and (b) show the UV–vis diffuse reflectance spectrum and the corresponding absorbance spectrum of as-prepared Sb_2Se_3 rods. Based on these data, and according to the following formula:

$$\alpha = \sqrt{h\nu - E_g}/h\nu \tag{6}$$

where $h\nu$ is the corresponding phonon energy and α is the absorbance coefficient, we made a $(ahv)^2 \sim h\nu$ plot (figure 7(c)), from which the bandgap (E_g) can be derived to be 1.16 eV. This value is near the optimum value for photovoltaic conversion, suggesting that Sb_2Se_3 submicron rods may be very promising for applications in solar energy and photoelectronics [28]. Our results are similar to those reported in [25, 28].

4. Conclusions

A new microwave-assisted chemical method was developed to synthesize orthorhombic Sb_2Se_3 rods with diameters of 100–200 nm and 1D preferential growth along the (001) direction from antimony sodium tartrate and Se powder. The reaction mechanism was studied in detail in comparison with those of Bi_2Te_3 and Sb_2Te_3, and was found to be based on the polyol reducing process. The morphology of Sb_2Se_3 is mainly determined by its inherent anisotropic crystal structure. The differences in the properties of the elements (Bi and Sb, Se and Te) and the crystal structures of the compounds result in the differences in the synthesis mechanisms and the morphologies of Sb_2Se_3, Bi_2Te_3 and Sb_2Te_3. As-prepared Sb_2Se_3 has a suitable bandgap value (1.16 eV) for applications in photovoltaic conversion.

Acknowledgments

This work is supported by the National Natural Science Foundation of China (grant no. 20635020), the NSFC for

Creative Research Group (20821063) and the Natural Science Foundation of the Jiangsu Higher Education Institutions of China (grant no. 06KJB150061).

References

[1] Huang Y, Duan X F, Cui Y, Lauhon L J, Kim K H and Lieber C M 2001 *Science* **294** 1313
[2] Bachtold A, Hadley P, Nakanishi T and Dekker C 2001 *Science* **294** 1317
[3] Yu Y, Jin C H, Wang R H, Chen Q and Peng L M 2005 *J. Phys. Chem.* B **109** 18772
[4] Huynh W U, Dittmer J J and Alivisatos A P 2002 *Science* **295** 2425
[5] Duan X, Huang Y, Cui Y, Wang J and Lieber C M 2001 *Nature* **409** 66
[6] Goldberger J, Sirbuly D J, Law M and Yang P 2005 *J. Phys. Chem.* B **109** 9
[7] Rao C N R, Deepak F L, Gundiah G and Govindaraj A 2003 *Prog. Solid State Chem.* **31** 5
[8] Xia Y, Yang P, Sun Y, Wu Y, Mayers B, Gates B, Yin Y, Kim F and Yan H 2003 *Adv. Mater.* **15** 353
[9] Li Y D, Li X L, Deng Z X, Zhou B C, Fan S S, Wang J W and Sun X M 2002 *Angew. Chem. Int. Edn* **41** 333
[10] Wang X and Li Y D 2002 *Chem. Commun.* 764
[11] Zhou B and Zhu J J 2006 *Nanotechnology* **17** 1763
[12] Fernández A M and Merino M G 2000 *Thin Solid Films* **366** 202
[13] Zheng X, Xie Y, Zhu L, Jiang X, Jia Y, Song W and Sun Y 2002 *Inorg. Chem.* **41** 455
[14] Rosi F D, Abeles B and Jensen R V 1959 *J. Phys. Chem. Solids* **10** 191
[15] Rajapure K, Lokhande C and Bhosele C 1997 *Thin Solid Films* **311** 114
[16] Kim I 2000 *Mater. Lett.* **43** 221
[17] Platakis N S and Gatos H C 1972 *Phys. Status Solidi* a **13** K1
[18] Arivuoli D, Gnanam F D and Ramasamy P 1988 *J. Mater. Sci. Lett.* **7** 711
[19] Christian P and O'Brien P 2005 *J. Mater. Chem.* **15** 4949
[20] Shen G Z, Chen D, Tang K B, Jiang X and Qian Y T 2003 *J. Cryst. Growth* **252** 350
[21] Wang D, Yu D, Shao M, Yu W and Qian Y 2002 *Chem. Lett.* **31** 1056
[22] Wang D, Yu D, Shao M, Xing J and Qian Y 2003 *Mater. Chem. Phys.* **82** 546
[23] Wang J, Deng Z and Li Y 2002 *Mater. Res. Bull.* **37** 495
[24] Xie Q, Liu Z, Shao M, Kong L, Yu W and Qian Y 2003 *J. Cryst. Growth* **252** 570
[25] Chen M and Gao L 2005 *Mater. Res. Bull.* **40** 1120
[26] Wang D, Yu D, Mo M, Liu X and Qian Y 2003 *J. Cryst. Growth* **253** 445
[27] Wang D, Song C, Fu X and Li X 2005 *J. Cryst. Growth* **281** 611
[28] Yu Y, Wang R H, Chen Q and Peng L M 2006 *J. Phys. Chem.* B **110** 13415
[29] Zhang Y X, Li G H, Zhang B and Zhang L D 2004 *Mater. Lett.* **58** 2279
[30] Chen M H and Gao L 2005 *J. Inorg. Mater.* **20** 1343
[31] Ma X C, Zhang Z, Wang X, Wang S T, Xu F and Qian Y T 2004 *J. Cryst. Growth* **263** 491
[32] Zhou B, Zhao Y, Pu L and Zhu J J 2006 *Mater. Chem. Phys.* **96** 192
[33] Zhou B, Ji Y, Yang Y F, Li X H and Zhu J J 2008 Rapid microwave-assisted synthesis of single-crystalline Sb_2Te_3 hexagonal nanoplates *Cryst. Growth Des.* **8** 4394–7
[34] Zhou B, Hong J M and Zhu J J 2005 *Mater. Lett.* **59** 3081
[35] Zhou B, Hong J M and Zhu J J 2008 *Chem. Lett.* **37** 730–1
[36] Lu W, Ding Y, Chen Y, Wang Z L and Fang J 2005 *J. Am. Chem. Soc.* **127** 10112
[37] Shi W D, Yu J B, Wang H S and Zhang H J 2006 *J. Am. Chem. Soc.* **128** 16490
[38] Black E M, Conwell L S and Spencer C W 1957 *J. Phys. Chem. Solids* **2** 240
[39] Tideswell N W, Kruse F H and McCullough J D 1957 *Acta Crystallogr.* **10** 99